

On the mixed-mode crack propagation in FGMs plates: comparison of different criteria

Benamara Nabil^{*1}, Boulenouar Abdelkader^{1a}, Aminallah Miloud^{1b} and Benseddiq Noureddine^{2c}

¹Laboratory of Materials and Reactive Systems, Mechanical Engineering Department, Djillali Liabes University of Sidi Bel-Abbes, BP. 89, City Larbi Ben M'hidi, 22000, Algeria

²Mechanics Laboratory of Lille, CNRS UMR 8107, Ecole Polytech'Lille, University of Lille, France

(Received September 28, 2015, Revised November 19, 2016, Accepted December 13, 2016)

Abstract. Modelling of a crack propagating through a finite element mesh under mixed mode conditions is of prime importance in fracture mechanics. In this paper, two crack growth criteria and the respective crack paths prediction in functionally graded materials (FGM) are compared. The maximum tangential stress criterion (σ_θ -criterion) and the minimum strain energy density criterion (S-criterion) are investigated using advanced finite element technique. Using Ansys Parametric Design Language (APDL), the variation continues in the material properties are incorporated into the model by specifying the material parameters at the centroid of each finite element. In this paper, the displacement extrapolation technique (DET) proposed for homogeneous materials is modified and investigated, to obtain the stress intensity factors (SIFs) at crack-tip in FGMs. Several examples are modeled to evaluate the accuracy and effectiveness of the combined procedure. The effect of the defects on the crack propagation in FGMs was highlighted.

Keywords: functionally graded materials; maximum tangential; strain energy density; crack propagation; displacement extrapolation technique; stress intensity factor

1. Introduction

Functionally graded materials (FGMs) are new multifunctional composites with smoothly varying volume fractions of constituent materials, which leads to a non-uniform microstructure with continuously graded macroproperties. FGMs possess material non-homogeneity with regard to thermomechanical and strength related properties including yield strength, fatigue and creep behavior, and fracture toughness. These materials were investigated to take advantage of ideal behavior of its material constituents. The prediction of fracture parameters for graded structures, generically termed functionally graded materials (FGMs), has received considerable attention over the last decade. There have been several attempts to study mixed mode fracture in FGMs and to determine whether fracture criteria developed for homogeneous materials are also valid for FGMs: Kidane *et al.* (2010) studied mixed-mode dynamic crack growth behavior in FGMs under thermo-mechanical loading. Using the minimum strain-energy density criterion and the

maximum circumferential stress criterion, the crack growth direction for various crack-tip speeds, non-homogeneity coefficients and temperature fields are determined. Ma *et al.* (2010) studied numerical simulation of mixed-mode crack propagation in FGMs by means of extended finite element Method (XFEM). Determination of the crack growth direction is based on a specific fracture criterion, using the assumption of local homogenization of asymptotic crack-tip fields in FGMs. Kim and Paulino (2007) investigated FE method with mesh refinement techniques and interaction integral method (M-integral) to simulate the mixed-mode crack growth in FGMs, using maximum hoop stress (Erdogan and Sih 1963), maximum energy release rate (Hussain *et al.* 1993) and minimum strain energy density (Sih 1974). Kim and Paulino (2005) studied the fracture behavior of FGMs under mechanical loading by performing automatic simulation of the crack propagation FGM through remeshing algorithm in conjunction with the finite element method. Crack trajectories obtained by the maximum energy release rate criterion proposed. Hosseini *et al.* (2013) implemented a computational method based on the extended finite element method (XFEM) and the maximum energy release rate criterion for crack propagation analysis of isotropic and orthotropic FGMs. Becker *et al.* (2001) investigated finite crack kinking by considering a hyperbolic-tangent material gradation with steep gradient of Young's modulus. They used the maximum energy release rate (Palaniswamy and Knauss 1978) and $K_{II}=0$ (Cotterell and Rice 1980) criteria. Kim and Paulino (2004) used the maximum energy release rate criterion proposed by Hussain *et al.* (1993) for homogeneous materials to check crack initiation condition

*Corresponding author, Ph.D.

E-mail: benamara96@yahoo.fr

^aProfessor

E-mail: aeq_boulenouar@yahoo.fr

^cProfessor

E-mail: aminallahm@yahoo.fr

^dProfessor

E-mail: noureddine.benseddiq@univ-lille1.fr

and to determine crack initiation angles in plate FGM under mixed-mode and non-proportional loading. Benamara *et al.* (2017) analyzed the mixed mode crack propagation in the FGM plate using the strain energy density approach. Lee and Erdogan (1995) calculated the effect of modulus gradient on the angle of maximum hoop stress near the free edge of a graded joint and discussed the implications on the direction of fracture initiation. Gu and Asaro (1997) investigated crack deflection in brittle FGMs by considering exponential gradation perpendicular to the crack, and used the $K_{II}=0$ criterion. Burlayenko *et al.* (2016) analyzed the crack growth in the FGM plate under thermal shock using the virtual crack closure technique VCCT. It is shown that the crack lengths are influenced by the material gradient profile of the functionally graded plate. Kim (2003) performed numerical simulation of mixed mode crack propagation in FGMs, and investigated the effect of material gradation on crack trajectory and critical loads. EL-Desouky and EL-Wazery (2013) investigated the maximum principle stress criterion to predict the mixed-mode fracture of FGMs and non-graded specimens. It is shown that initial propagation direction of the non-graded composites and FGM specimens was approximately predicted as the range (7-15°) according to MPS theory and was in good agreement with the estimated propagation direction of the experimental result.

This paper based on 2D mixed-mode crack propagation in FGMs using the finite element method (FEM) and compares the performance of some fracture criteria ($\sigma(\theta)$ and $S(\theta)$) to predict the crack trajectory in cracked FGMs. The displacement extrapolation technique (DET) was used, to determine the SIFs around the crack-tip. In this investigation, the effect of inclusions and cavities on the crack trajectories in FGMs was examined.

The present paper is organized as follows: Section 2 presents the crack growth criteria investigated for this study. Section 3 addresses the numerical evaluation of SIFs. Section 4 explains the methodology of crack extension proposed for FGMs, and section 5 provides some numerical applications for FE evaluation of SIFs and crack propagation simulation. Finally, section 6 concludes the present investigation.

2. Crack direction criteria

2.1 Maximum tangential stress criterion (σ_θ -criterion)

For this approach, the maximum tangential stress $\sigma_{\theta,max}$ is taken as the criterion of failure in terms of critical stress σ_c . The maximum tangential stress criterion was the first one presented by Erdogan and Sih (1963). It is assumed that the onset of crack propagation occurs when the maximum value of tangential stress reaches a critical stress value σ_c of the material under a simple tension test. Therefore, the condition for crack extension can be given by

$$\sigma_{\theta,max} = \sigma_c \quad (1)$$

Under the combination of modes I and II loadings in polar coordinates, the tangential stress, as shown in Fig. 1, can be defined by the following equation

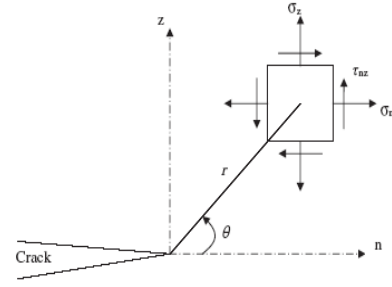


Fig. 1 Definition of stress state at the crack-tip

$$\sigma_\theta = \frac{1}{2}(\sigma_n + \sigma_z) - \frac{1}{2}(\sigma_n - \sigma_z) \cos 2\theta - \tau_{nz} \sin 2\theta \quad (2)$$

The local stresses on an element near the crack-tip for 2D stress state, could be expressed in terms of the spherical coordinates (r, θ), as shown in Fig. 1, and they were given by Sih (1975) as

$$\sigma_n = \frac{1}{\sqrt{2\pi r}} \left[K_I \cos \frac{\theta}{2} \left(1 - \sin \frac{\theta}{2} \sin \frac{3\theta}{2} \right) - K_{II} \sin \frac{\theta}{2} \left(2 + \cos \frac{\theta}{2} \cos \frac{3\theta}{2} \right) \right] \quad (3)$$

$$\sigma_z = \frac{1}{\sqrt{2\pi r}} \left[K_I \cos \frac{\theta}{2} \left(1 + \sin \frac{\theta}{2} \sin \frac{3\theta}{2} \right) + K_{II} \sin \frac{\theta}{2} \cos \frac{\theta}{2} \cos \frac{3\theta}{2} \right] \quad (4)$$

$$\tau_{nz} = \frac{1}{\sqrt{2\pi r}} \left[K_I \sin \frac{\theta}{2} \cos \frac{\theta}{2} \cos \frac{3\theta}{2} + K_{II} \cos \frac{\theta}{2} \left(1 - \sin \frac{\theta}{2} \sin \frac{3\theta}{2} \right) \right] \quad (5)$$

$$\sigma_t = \nu(\sigma_n + \sigma_z) = \frac{2\nu}{\sqrt{2\pi r}} \left[K_I \cos \frac{\theta}{2} - K_{II} \sin \frac{\theta}{2} \right] \quad \text{plan strain} \quad (6)$$

$$\sigma_t = 0 \quad \text{plan stress} \quad (7)$$

where K_I and K_{II} are the stress intensity factors (SIFs) under mode-I and mode-II loading, respectively.

Substituting the singular solution of Eqs. (3)-(7) into Eq. (2) and after rearranging, the tangential stress can be expressed as follows

$$\sigma_\theta = \frac{K_I}{\sqrt{2\pi r}} \left\{ \cos \frac{\theta}{2} \left[1 + \sin \frac{\theta}{2} \left(\sin \frac{3\theta}{2} \cos \frac{4\theta}{2} - \cos \frac{3\theta}{2} \sin \frac{4\theta}{2} \right) \right] - \frac{K_{II}}{\sqrt{2\pi r}} \left\{ \sin \frac{\theta}{2} \left(1 - \cos \frac{4\theta}{2} \right) + \cos \frac{\theta}{2} \left[\sin \frac{4\theta}{2} - \sin \frac{\theta}{2} \left(\cos \frac{3\theta}{2} \cos \frac{4\theta}{2} + \sin \frac{3\theta}{2} \sin \frac{4\theta}{2} \right) \right] \right\} \right\} = \frac{1}{\sqrt{2\pi r}} f_\theta(K_I, K_{II}, \theta) \quad (8)$$

where θ is the crack propagation direction. Therefore, Eq. (1) can be expressed as follows

$$\frac{1}{\sqrt{2\pi r}} f_{\theta,max}(K_I, K_{II}, \theta) = \sigma_c \quad (9)$$

The σ_θ -criterion assumed that the angle θ_0 of the crack propagation direction can be obtained by maximizing the above σ_θ value, i.e.

$$\begin{aligned} \left(\frac{\partial \sigma_\theta}{\partial \theta}\right)_{\theta=\theta_0} &= \frac{1}{\sqrt{2\pi r}} \left(\frac{\partial f_\theta}{\partial \theta}\right)_{\theta=\theta_0} = 0, \\ \left(\frac{\partial^2 \sigma_\theta}{\partial \theta^2}\right)_{\theta=\theta_0} &< 0 \end{aligned} \quad (10)$$

2.2 Minimum strain energy density criterion (S-criterion)

Sih (1974) proposed the strain energy density approach. It states that the direction of crack initiation coincides with the direction of minimum strain energy density, along a constant radius around the crack-tip. This criterion is the only one that illustrates dependence of crack initiation angle on the material elastic properties represented by the Poisson's ratio, ν and the state of the stress Erdogan and Sih (1963).

It is assumed that the onset of crack propagation occurs when the minimum value of S_{\min} reaches a critical value S_c .

For this criterion, the condition for crack extension is given by

$$S_{\min} = S_c \quad (11)$$

Under mixed modes I+II loadings, the strain energy density factor S was given by Sih (1973) as follows

$$S = a_{11}K_I^2 + 2a_{12}K_IK_{II} + a_{22}K_{II}^2 \quad (12)$$

Where: a_{ij} are constants which vary with the angles θ measured from the crack-tip, have been given by Sih (1973) as follows

$$a_{11} = \frac{\kappa + 1}{16\mu\kappa^2\cos\theta} \left[2(1 - 2\nu) + \frac{\kappa - 1}{\kappa} \right] = \frac{1}{\cos\theta} f_{11} \quad (13)$$

$$a_{12} = \frac{(\kappa^2 - 1)^{1/2}}{8\mu\kappa^2\cos\theta} \left[\frac{1}{\kappa} - (1 - 2\nu) \right] = \frac{1}{\cos\theta} f_{12} \quad (14)$$

$$\begin{aligned} a_{22} &= \frac{1}{16\mu\kappa^2\cos\theta} \left[4(1 - \nu)(\kappa - 1) + \frac{1}{\kappa}(\kappa + 1)(3 - \kappa) \right] \\ &= \frac{1}{\cos\theta} f_{22} \end{aligned} \quad (15)$$

therefore, the strain energy density factor S can be expressed as follows

$$S = \frac{1}{\cos\theta} (f_{11}K_I^2 + 2f_{12}K_IK_{II} + f_{22}K_{II}^2) = f_s(K_I, K_{II}, \theta) \quad (16)$$

where the angle θ is the direction of crack propagation. Therefore Eq. (11) becomes

$$f_{s,\min}(K_I, K_{II}, \theta) = S_c \quad (17)$$

This criterion assumed that the crack will begin to extend in certain direction in which the strain energy density factor possesses a relative minimum value, i.e.

$$\left(\frac{\partial S}{\partial \theta}\right)_{\theta=\theta_0} = 0, \quad \left(\frac{\partial^2 S}{\partial \theta^2}\right)_{\theta=\theta_0} > 0 \quad (18)$$

3. Numerical calculation of stress intensity factors SIFs

In LEFM, the SIFs are the important parameters used in various modes. Several techniques have been proposed to obtain these parameters for homogeneous and non-homogeneous materials, such as the displacement correlation technique (DCT) (Sabuncuoglu *et al.* 2012, Shih *et al.* 1967, Kim *et al.* 2002), the modified crack-closure integral MCC (Rybicki and Kanninen 1977, Kim and Paulino 2002), the interaction integral (Topal and Dag 2013, Dag 2006, Dag *et al.* 2010, Kim and Paulino 2003a, 2003b, 2004, 2007) and the stress correlation (Raju *et al.* 1979). In this investigation, the displacement extrapolation technique (DET) used to calculate the SIFs K_I and K_{II} for homogeneous materials (Boulenouar *et al.* 2016, 2014, 2013a, 2013b, and Benouis *et al.* 2015) is modified to calculate the SIFs for non-homogeneous materials. For the FGMs, the SIFs K_I and K_{II} can be expressed as follows

$$K_I = \frac{E_{tip}}{3(1 + \nu_{tip})(1 + k_{tip})} \sqrt{\frac{2\pi}{L}} \left[4(v_b - v_d) - \frac{(v_c - v_e)}{2} \right], \quad (19a)$$

$$K_{II} = \frac{E_{tip}}{3(1 + \nu_{tip})(1 + k_{tip})} \sqrt{\frac{2\pi}{L}} \left(4(u_b - u_d) - \frac{(u_c - u_e)}{2} \right), \quad (19b)$$

where:

E_{tip} and ν_{tip} are the Young's modulus and the Poisson's ratio at the crack-tip location, respectively. $\kappa_{tip} = 3 - 4\nu_{tip}$ for plane strain, $\kappa_{tip} = (3 - \nu_{tip}) / (1 + \nu_{tip})$ for plane stress.

u_i and v_i ($i=b, c, d$ and e) are the nodal displacements at nodes b, c, d and e in x and y directions, respectively (Fig. 2).

In this paper, the special quarter point finite elements proposed by Barsoum (1974) are used to obtain a better approximation of the field near crack-tip. As shown in Fig. 2, the mid-side node of the element in the crack-tip is moved to 1/4 of the length of the element.

4. Methodology of crack propagation modelling

The main objective of this study is to evaluate mixed mode stress intensity factors K_I and K_{II} for mixed-mode fracture analysis under mechanical loading conditions by considering isotropic FGMs. For this purpose, a two

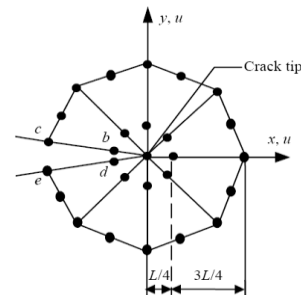


Fig. 2 Special quarter point finite elements proposed by Barsoum used for DET

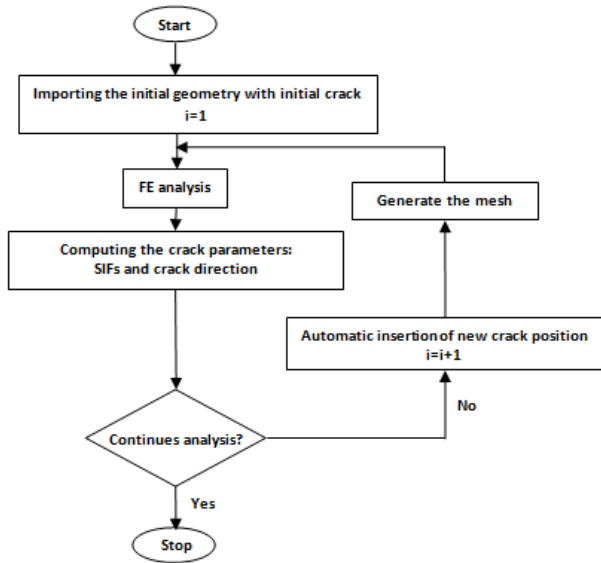


Fig. 3 Algorithm of the main operations for the crack propagation modeling

dimensional finite element model is developed using finite element software, ANSYS.

In the technical literature, two basic approaches are utilized to compute the material properties of FGMs. In the first approach, the physical properties are represented by certain continuous functions of spatial coordinates. In the second approach, micromechanics models are used to estimate the material parameters. In this paper, an APDL subroutine is developed for the implementation of material property variations of FGM's. The material properties (E_i and ν_i) are specified for each element (i) at its centroid.

In order to simulate the stress concentration at the crack tip more accurately displacement extrapolation technique (DET) subroutines, the mesh is skewed at the crack tip and the 8-noded quadrilaterals are collapsed to triangles around the crack tip. In order to examine the accuracy of the model, calculated SIFs are compared with those available in the literature.

In this study, two crack direction criteria (σ_θ and S_θ) are investigated to determine the crack direction θ . At each crack increment length Δa , the angle θ is evaluated as a function of stress intensity factors K_I and K_{II} (using Eqs. (10) and (18)). The mathematical solution of these equations is assured using the computer code MAPLE 6.0.

Generally, the crack propagation in FGMs is characterized by successive propagation steps. Each step consists of:

1. Setting the geometrical with initial crack and input material properties data of the problem.
2. Discretization of the FE model by plane2 elements 'PLANE183'.
3. Mesh definition; 3. Mesh definition: the mesh and the re-mesh operation of FGM plate are given automatically by Ansys code.
4. FE calculation.
5. Computation of SIFs K_I and K_{II} (using Eqs. (19a) and (19b)).
6. Computation of crack growth direction.

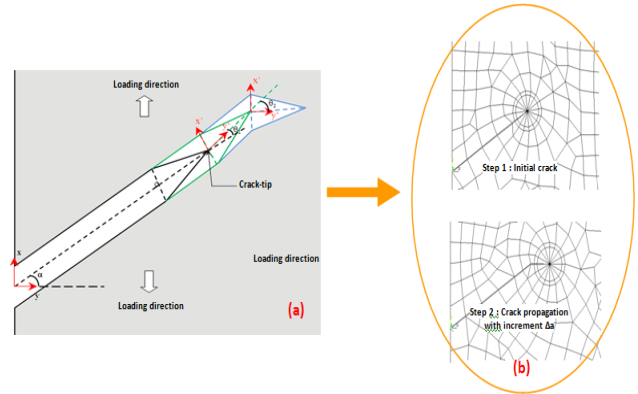


Fig. 4 (a) Crack propagation mechanism proposed in this investigation; (b) FE modeling

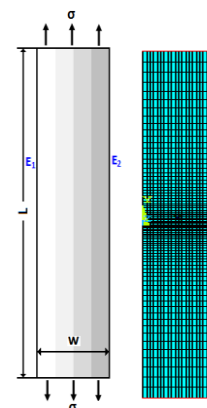


Fig. 5 Configuration for uncracked strip under under tension loading

7. Continues analysis? If yes, go to step 8. If no, go to step 9.
8. Stop.
9. Automatic delete of the crack segment and insertion of the new crack-tip position.
10. Return to Step 3

Fig. 3 describes the flowchart for predicting the crack growth trajectory based on the combination of the FE analysis and the crack direction criteria. Fig. 4 shows the crack propagation mechanism proposed in this work.

5. Numerical analysis and validation

The FGM can be defined by the variation of the volume fractions. The majority of the researchers employ the power law function, the exponential function, or the sigmoid function to describe the volume fractions. In present investigation, an APDL subroutine is developed for the implementation of material property variations of FGM's using the exponential model. The material properties are specified for each element at its centroid.

5.1 Stress distribution for uncracked strip under tension

The basic geometry of the FGM uncracked strip

considered in this study is shown in Fig. 5(a). The plate is subjected to uni-axial loading at the both ends. The elastic modulus for FGMs plate was assumed to follow an exponential function given by

$$E(x) = E_1 \exp(\lambda x), \quad 0 \leq x \leq w \quad (20)$$

with $E = E_1(0)$, $E = E_2(w)$, and $\lambda = Ln(E_2/E_1)$.

Fig. 5(b) shows a typical mesh model of FGM plate with 1600 elements and 5000 nodes. In this study, the following data were used:

$\sigma = 1$, $E_1 = 1$; $E_2/E_1 = (1, 2, 5, 10 \text{ and } 20)$; $\nu = 0.3$ and $L/w = 8$.

Fig. 6 shows the evolution of stress distributions σ_{yy} for uncracked plate under tension loading. The results obtained are compared with FEM results obtained by Kim and Paulino (2002). This comparison shows that the two results agree within plotting accuracy. Thus such excellent results validate the present FEM implementation for elastic FGMs.

5.2 FE evaluation of SIFs

In this section, the geometry of the single edge cracked FGM plate with an initial crack of length a is considered for 2-Dimensional FE analysis (Fig. 7(a)). This geometry was originally investigated by Erdogan and Wu (1997), and it is one of the few analytical solutions available for fracture in FGMs. In this investigation, the following data were used under plane strain condition:

$\sigma = 1$, $E_1 = 1$; $E_2/E_1 = (0.1, 0.2, 1, 5 \text{ and } 10)$; $\nu = 0.3$; $a/w = 0.2, 0.3, 0.5 \text{ and } 0.6$; $L/w = 8$.

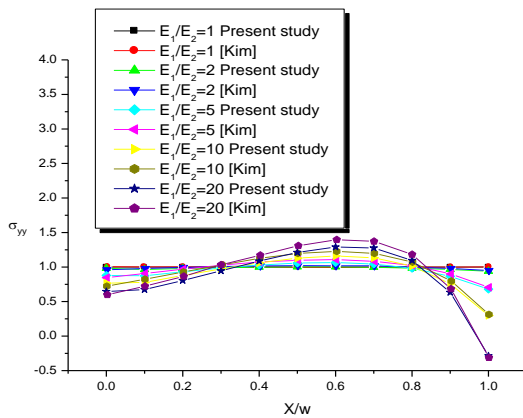


Fig. 6 Stress distribution σ_{yy} for uncracked strip

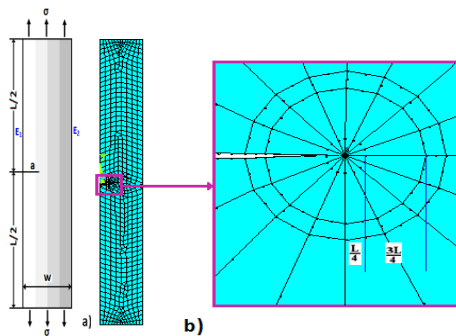


Fig. 7 (a) Geometry and boundary conditions of FGM plate; (b) Singular element around the crack-tip ($a/w = 0.2$)

Fig. 7(b) shows the mesh discretization of cracked FGMs plate with 710 elements and 2241 nodes. The special quarter point finite elements proposed by Barsoum (1974) are used for modeling the singular field around the crack-tip.

Table I compare the normalized SIFs obtained by DET with:

1. The analytical solution obtained by Erdogan and Wu (1997),
2. The numerical results of Kim and Paulino (2002b) using two techniques: J^* -Integral method and the modified crack-closure (MMC) integral method and,
3. The results obtained by Chen *et al.* (2000) using the element free Galerkin (EFG) method.

The results obtained indicate good agreement between ours results and other author's solution for this example. These results allow us to conclude that the displacement extrapolation technique modified for non-homogeneous materials, correctly described the stress-strain field around the crack-tip.

5.3 Crack propagation simulation in FGM

In this section, two examples are presented (single edge cracked plate with one hole and another cracked plate with an inclusion). For these examples, the variation of the elastic modulus for FGM was modeled by Eq. (20).

5.3.1 Single edge cracked FGM plate with one hole

This geometry was considered to study the effect of defect on the crack extension in FGMs. Fig. 8(a) shows the geometry of the single edge cracked plate with one hole. This plate is simply fixed at the bottom edge and loaded by uni-axial traction along the top edge. The geometry was meshed using 8-node quadratic elements and triangular elements concentric at crack-tip (Fig. 8(b)). The determination of SIFs, direction angle and crack growth path are made under plane stress problem. For first step of crack propagation, the number of element used in this analysis is 1144 elements with 3570 nodes.

The numerical calculations obtained are compared with other results, for a homogeneous material case (with $E_2/E_1 = 1$). Fig. 9 shows the final configuration corresponding to the last position of crack-tip for the results obtained by Bouchard *et al.* (2000), Rashid (1988), and that obtained in present study. The crack propagation paths obtained are semicircles between them.

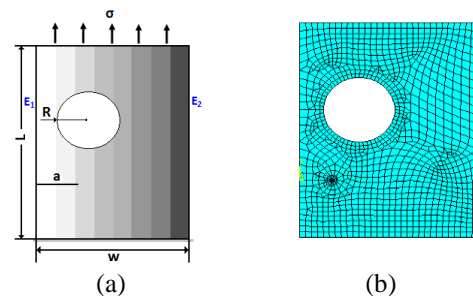


Fig. 8 (a) Geometry model of cracked FGMs plate with one hole and (b) typical FE mesh for initial configuration

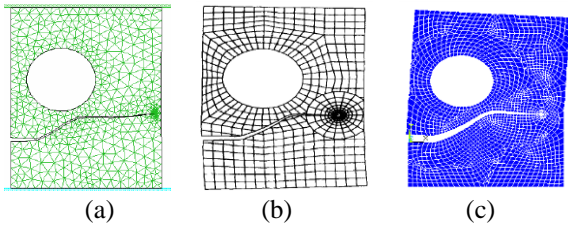


Fig. 9 Final configuration corresponding to the last position of crack-tip (with $E_2/E_1=1$): (a) Bouchard *et al.* (2000), (b) Rashid (1988) and (c) Present study

Table 1 Normalized SIFs for edge cracked FGM plate for: $a/w=0.2, 0.3, 0.5$ and 0.6

Method	E_2/E_1	a/w				
		0.2	0.3	0.4	0.5	0.6
Erdogan and Wu (1997)	0.1	1.296	1.858	2.569	3.570	5.188
	0.2	1.395	1.839	2.443	3.326	4.761
	1	N/A	N/A	N/A	N/A	N/A
	5	1.131	1.369	1.748	2.365	3.445
	10	1.001	1.229	1.588	2.176	3.212
Kim and Paulino (2002b) J^* Integral	0.1	1.284	1.846	2.544	3.496	4.962
	0.2	1.39	1.831	2.431	3.292	4.669
	1	1.358	1.658	2.11	2.822	4.03
	5	1.132	1.37	1.749	2.366	3.448
	10	1.003	1.228	1.588	2.175	3.212
Kim and Paulino (2002b) MMC	0.1	1.28	1.832	2.523	3.470	4.921
	0.2	1.38	1.818	2.411	3.268	4.632
	1	1.358	1.649	2.097	2.806	4.005
	5	1.129	1.371	1.744	2.36	3.437
	10	1.001	1.234	1.582	2.174	3.207
Chen <i>et al.</i> (2000) EPG Method	0.1	1.366	1.926	2.658	3.666	5.243
	0.2	1.455	1.897	2.529	3.443	4.926
	1	1.408	1.698	2.178	2.933	4.237
	5	1.158	1.392	1.794	2.446	3.611
	10	1.032	1.249	1.614	2.223	3.337
Present study DET	0.1	1.312	1.871	2.576	3.539	5.011
	0.2	1.406	1.850	2.455	3.328	4.714
	1	1.372	1.667	2.125	2.847	4.070
	5	1.135	1.375	1.758	2.385	3.486
	10	1.006	1.234	1.598	2.194	3.251

Fig. 10 shows the evolution of normalized SIFs K_{I} ($K_I/\sigma(\pi a)^{0.5}$) and K_{II} ($K_{II}/\sigma(\pi a)^{0.5}$) during crack propagation extension obtained in FGM plate using the σ_θ -criterion. These results are compared with those obtained by S -criterion. The plotted curves show a good agreement between the two approaches.

Fig. 11 compares the crack trajectories obtained by σ_θ and S_θ criteria due to the presence of the hole. The two approaches give good results on the crack propagation path and the results between them are very close.

Fig. 12 illustrates four steps for crack extension in FGM plate using the σ_θ -criterion. This crack would move in a straight path if there was no hole at the plate for opening-mode (mode-I) loading (Fig 12(a)). However, due to the presence of the default, the crack did not follow a straight line path, but curved towards the hole as shown in Fig. 12(b). This was due to the stress concentration effect; cracks are likely to initiate at a hole boundary. Once the crack-tip has moved beyond the default, the crack reoriented horizontally in the mode I loading as shown in

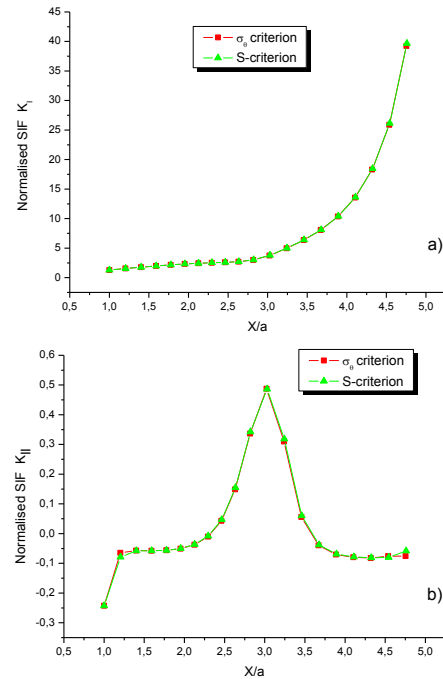


Fig. 10 Evolution of normalized SIFs during crack extension in FGM plate with one hole: (a) Normalized K_I and (b) Normalized K_{II}

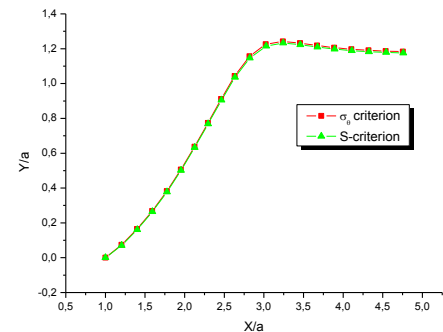


Fig. 11 Crack trajectories comparison

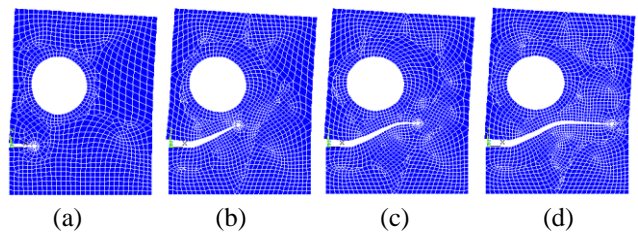


Fig. 12 Four steps of crack propagation trajectory for a single edge cracked FGM plate with one hole

Figs. 12(c) and 12(d).

Fig. 13 shows the crack trajectories obtained for homogeneous and FGMs plates obtained by σ_θ -criterion. One can notice the same crack propagation behavior for both plates but the two crack paths are different from each other. This may explain the fact that the stress distribution around the hole is different for the two plates, which may influence directly on the propagation trajectory (Benamara *et al.* 2017).

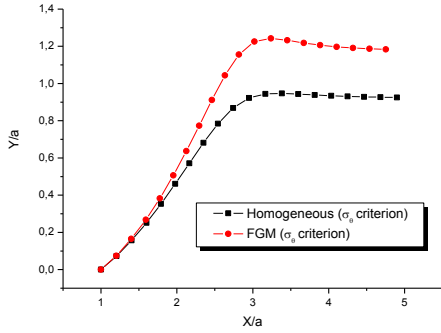


Fig. 13 Positions of the crack-tip obtained for homogeneous and FGM plate (σ_θ -criterion)

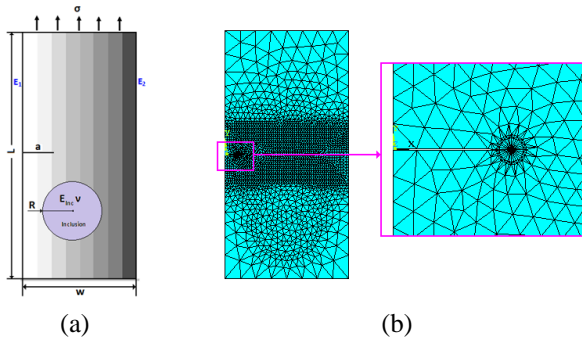


Fig. 14 (a) Geometrical model of the cracked FGM plate with an inclusion and (b) final mesh for initial configuration

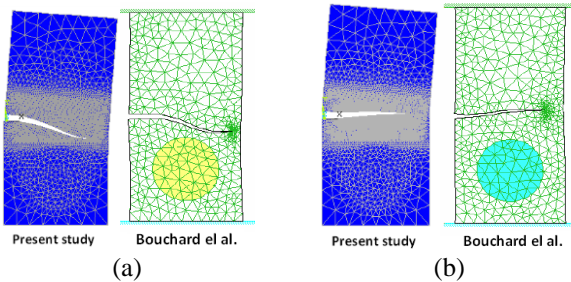


Fig. 15 Final configuration corresponding to the last position crack-tip: (a) $E_{inc}/E_1=0.1$, (b) $E_{inc}/E_2=10$

5.3.2 Cracked FGM plate with an inclusion

In what follows, we propose to study the inclusion effect on the crack path in FGMs. For this purpose, we considered a pre-cracked FGM plate with a circular inclusion, having the following dimensions: $W/R=3.5$ and $L/W=0.5$ (Fig. 14(a)). The FGM plate is fixed at the bottom edge and loaded by uniform tension along the top edge. A typical FE model of the FGM plate with an inclusion is shown in Fig. 14(b). The crack propagation prediction is performed under plane stress conditions. For first step of crack propagation, the FGM plate was modeled by 4098 elements with 8309 nodes.

The mechanical properties of the FGM plate are given by Eq. (20). The inclusion considered is characterized by its Poisson's ratio $\nu_{inc}=\nu=0.3$ and Young's modulus E_{inc} .

Firstly, our numerical model was to check for a homogeneous material and the results obtained are compared with the numerical results obtained by Bouchard

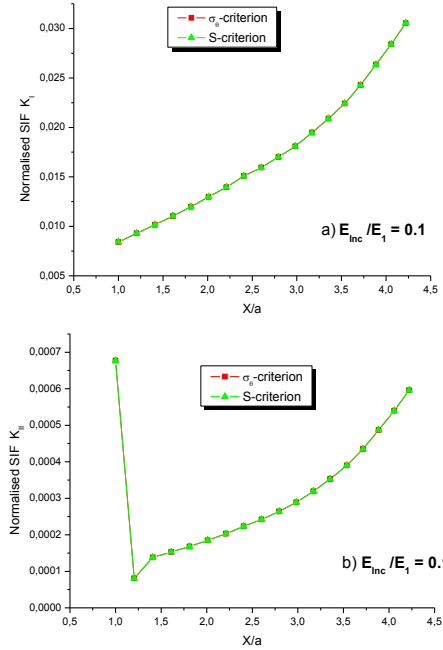


Fig. 16 Evolution of normalized SIFs during crack extension in FGM plate with an inclusion ($E_1=1$, $E_2=10$ and $E_{inc}/E_2=0.1$): (a) Normalized K_I and (b) Normalized K_{II}

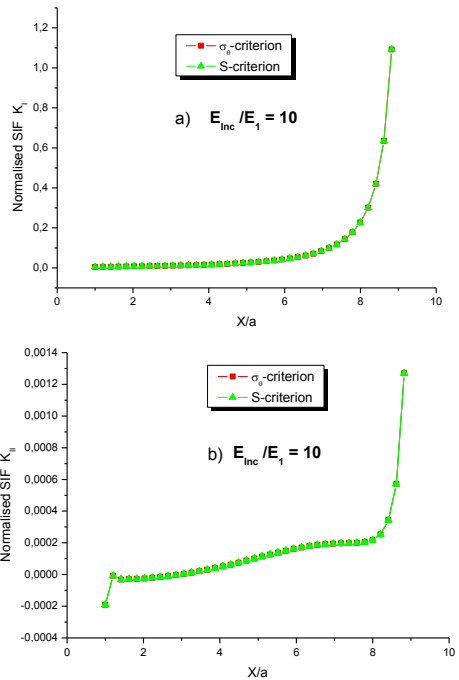


Fig. 17 Evolution of normalized SIFs during crack extension in FGM plate with an inclusion ($E_1=1$, $E_2=10$ and $E_{inc}/E_2=10$): (a) Normalized K_I and (b) Normalized K_{II}

et al. (2003). The crack propagation trajectories are obtained for two cases (Benamara *et al.* 2017):

a) $E_{inc}/E_1 = 0.1$ with $E_1=1$, $E_2=10$ (Fig. 15(a)),

b) $E_{inc}/E_2 = 10$ with $E_1=1$, $E_2=10$ (Fig. 15(b)).

The predicted crack propagation trajectory of the present study is quite similar to that obtained by Bouchard *et al.* (2003).

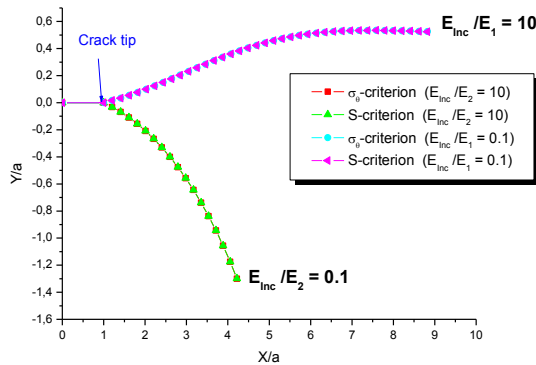


Fig. 18 Crack trajectories comparison in cracked FGM plate with an inclusion

For FGM plate case, the evolution of normalized SIFs K_I and K_{II} during crack propagation obtained by σ_θ and S_θ criteria, for two cases $E_{inc} < E_1$ (with $E_{inc}/E_1 = 0.1$) and $E_{inc} > E_2$ (with $E_{inc}/E_2 = 10$) is shown in Figs. 16 and 17, respectively. The plotted curves show a good agreement between these two approaches.

For two cases, Fig. 17 shows the prediction of the crack propagation path using the σ_θ -criterion. A calculation made by our numerical techniques shows that:

- If $E_{inc}/E_1 = 0.1$, the inclusion is less rigid than the FGM, the crack is attracted to the inclusion (Fig. 17(a)).
- If $E_{inc}/E_2 = 10$, the inclusion is more rigid than the FGM, the crack is moving away from the inclusion (Fig. 17(b)).

Fig. 18 compares the crack trajectories obtained by the two approaches due to the presence of inclusion. For the two cases, the two criteria give good results on the crack propagation path and the results between them are very close.

6. Conclusions

In this study, the quarter-point singular elements proposed by Barsoum are used to consider the singularity of stress and deformations fields at crack-tip in FGMs.

The displacement extrapolation technique was used to obtain the SIFs at crack-tip and to predict then the final crack trajectory by evaluation, for each propagation step, the kinked angle using two different crack growth criteria.

The SIFs for a single edge cracked plate was evaluated and compared with available analytical and numerical solutions. The comparison shows that our numerical techniques are capable of demonstrating the SIF evaluation. The methodology of crack propagation modeling proposed in this paper has been used successfully to predict the crack path in FGM plate contains holes and inclusion.

References

ANSYS, Inc. (2009), Programmer's Manual for Mechanical APDL, Release 12.1.

Barsoum, R.S. (1974), "On the use of isoparametric finite element

in linear fracture mechanics", *Int. J. Numer. Meth. Eng.*, **10**, 25-37.

Becker, T.L. Jr., Cannon, R.M. and Ritchie, R.O. (2001), "Finite crack kinking and T-stresses in functionally graded materials", *Int. J. Solid. Struct.*, **38**(32-33), 5545-5563.

Benamara, N., Boulououar, A. and Aminallah, M. (2017), "Strain energy density prediction of mixed-mode crack propagation in functionally graded materials", *Period. Polytech. Mech. Eng.* (in press)

Benouis, A., Boulououar, A., Benseddiq, N. and Serier, B. (2015), "Numerical analysis of crack propagation in cement PMMA, Application of SED approach", *Struct. Eng. Mech.*, **55** (1), 93-109.

Bouchard, P.O., Bay, F. and Chastel, Y. (2003), "Numerical modelling of crack propagation: automatic remeshing and comparison of different criteria", *Comput. Meth. Appl. Mech. Eng.*, **192**, 3887-3908.

Bouchard, P.O., Bay, F., Chastel, Y. and Tovenia, I. (2000), "A modified J-integral for functionally graded materials crack propagation modelling using an advanced remeshing", *Comput. Meth. Appl. Mech. Eng.*, **189**, 723-742.

Boulououar, A., Benouis, A. and Benseddiq, N. (2016), "Numerical modelling of crack propagation in cement PMMA: comparison of different criteria", *Mater. Res.*, **19**(4), 846-855.

Boulououar, A., Benseddiq, N. and Mazari, M. (2013a), "Strain energy density prediction of crack propagation for 2D linear elastic materials", *Theor. Appl. Frac. Mech.*, (67-68) 29-37.

Boulououar, A., Benseddiq, N. and Mazari, M. (2013b), "Two-dimensional numerical estimation of stress intensity factors and crack propagation in linear elastic analysis", *Eng. Technol. Appl.* **5**, 506-510.

Boulououar, A., Benseddiq, N., Mazari, M. and Benamara, N. (2014), "FE model for linear-elastic mixed mode loading: Estimation of sifs and crack propagation", *J. Theor. Appl. Mech.*, **52** (2), 373-383.

Burlayenko, V.N., Altenbach, H., Sadowski, T. and Dimitrova, S.D. (2016), "Computational simulations of thermal shock cracking by the virtual crack closure technique in a functionally graded plate", *Comput. Mater. Sci.*, **116**, 11-21.

Chen, J., Wu, L. and Du, S. (2000), "A modified J-integral for functionally graded materials", *Mech. Struct. Mach.*, **54**, 301-306.

Cotterell, B. and Rice, J.R. (1980), "Slightly curved or kinked cracks", *Int. J. Fract.*, **16**(2), 155-169.

Dag, S. (2006), "Thermal fracture analysis of orthotropic functionally graded materials using an equivalent domain integral approach", *Eng. Fract. Mech.*, **73**, 2802-2828.

Dag, S., Arman, E.E. and Yildirim, B. (2010), "Computation of thermal fracture parameters for orthotropic functionally graded materials using J_k -integral", *Int. J. Solid. Struct.*, **47**, 3480-3488.

EL-Desouky, A.R. and EL-Wazery, M.S. (2013), "Mixed mode crack propagation of Zirconia/Nickel functionally graded materials", *Int. J. Eng.*, **26**(8), 885-894.

Erdogan, F. and Sih, G.C. (1963), "On the crack extension in plates under plane loading and transverse shear", *J. Basic Eng.*, **85**, 519-27.

Erdogan, F. and Wu, B.H. (1997), "The surface crack problem for a plate with functionally graded properties", *ASME J. Appl. Mech.*, 449-456.

Gu, P. and Asaro, R.J. (1997), "Crack deflection in functionally graded materials", *Int. J. Solid. Struct.*, **34**(24), 3085-3098.

Hosseini, S.S., Bayesteh, H. and Mohammadi, S. (2013), "Thermo-mechanical XFEM crack propagation analysis of functionally graded materials", *Mater. Sci. Eng.-A*, **561**, 285-302.

Hussain, M.A., Pu, S.L. and Underwood, J. (1993), "Strain energy release rate for a crack under combined mode I and mode II",

- Eds. Paris, P.C. and Irwin, G.R., *Fracture Analysis*, ASTM STP 560, Philadelphia.
- Kidane, A., Chalivendra, V.B., Shukla, A. and Chona, R. (2010), "Mixed mode dynamic crack propagation in graded material under thermomechanical loading", *Eng. Fract. Mech.*, **77**, 2864-2880.
- Kim, J.H. (2003), "Mixed-mode crack propagation in functionally graded materials", Ph.D. Thesis, University of Illinois at Urbana-Champaign, Illinois.
- Kim, J.H. and Paulino, G.H. (2002), "Finite element evaluation of mixed mode stress intensity factors in functionally graded materials", *Int. J. Numer. Meth. Eng.*, **53**, 1903-1935.
- Kim, J.H. and Paulino, G.H. (2003 b), "The interaction integral for fracture of orthotropic functionally graded materials: evaluation of stress intensity factors", *Int. J. Solid. Struct.*, **40**, 3967-4001.
- Kim, J.H. and Paulino, G.H. (2003a), "Mixed-mode J-integral formulation and implementation using graded finite elements for fracture analysis of non-homogeneous orthotropic materials", *Mech. Mater.*, **35**, 107-128.
- Kim, J.H. and Paulino, G.H. (2004), "Simulation of crack propagation in functionally graded materials under mixed-mode and non-proportional loading", *Int. J. Mech. Mater. Des.*, **1**(1), 63-94.
- Kim, J.H. and Paulino, G.H. (2005), "Mixed-mode crack propagation in functionally graded materials", *Mater. Sci., Trans Tech Publ.*, **492**, 409-414.
- Kim, J.H. and Paulino, G.H. (2007), "On fracture criteria for mixed-mode crack propagation in functionally graded materials", *Mech. Adv. Mater. Struct.*, **14**, 227-244.
- Lee, Y.D. and Erdogan, F. (1994), "Residual/thermal stresses in FGM and laminated thermal barrier coatings", *Int. J. Fract.*, **69**(2), 145-165.
- Ma, L., Wang, Z.Y. and Wu, L.Z. (2010), "Numerical simulation of mixed-mode crack propagation in functionally graded materials", *Mater. Sci.*, **631-632**, 121-126.
- Palaniswamy, K. and Knauss, W.G. (1978), "On the problem of crack extension in brittle solids under general loading", Ed. Nemat-Nasser, S., *Mechanics Today*, Vol. **4**, Pergamon Press.
- Raju, I.S. and Newman, J.C. (1979), "Stress-intensity factors for a wide range of semi-elliptical surface cracks in finite-thickness plates", *Eng. Fract. Mech.*, **11**(4), 817-829.
- Rashid, M.M. (1988), "The arbitrary local mesh replacement method: An alternative to remeshing for crack propagation analysis", *Comput. Meth. Appl. Mech. Eng.*, **154**, 133-150.
- Rybicki, E.F. and Kanninen, M.F. (1977), "A finite element calculation of stress intensity factors by a modified crack closure integral", *Eng. Fract. Mech.*, **9**, 931-938.
- Sabuncuoglu, B., Dag, S. and Yildirim, B. (2012), "Three dimensional computational analysis of fatigue crack propagation in functionally graded materials", *Comput. Mater. Sci.*, **52**, 246-252.
- Shih, C.F., DeLorenzi, H.G. and German, M.D. (1967), "Crack extension modeling with singular quadratic isoparametric elements", *Int. J. Fract.*, **12**, 647-651.
- Sih, G.C. (1973), *Mechanics of Fracture I: a Special Theory of Crack Propagation*, Noordhoff International Publishing, Leyden.
- Sih, G.C. (1974), "Strain energy-density factor applied to mixed mode crack problem", *Int. J. Fract.*, **10**(3), 305-321.
- Sih, G.C. (1975), *Three dimensional crack problems, Mechanics of fracture*, V. 2, Noordhoff, Netherlands.
- Topal, S. and Dag, S. (2013), "Hygrothermal fracture analysis of orthotropic functionally graded materials using J_K -Integral-based methods", *Math. Probl. Eng.*, Article ID 315176, 11.